Biochimica et Biophysica Acta, 382 (1975) 322–335

BBA 76874

X-RAY DIFFRACTION STUDIES OF RETINAL RODS
I. STRUCTURE OF THE DISC MEMBRANE, EFFECT OF ILLUMINATION

MARC CHABRE

Biophysique, Département de Recherche Fondamentale, CEN-G, B.P. 85, 38041, Grenoble and Centre de Génétique Moléculaire, C.N.R.S., 91 Gif-sur-Yvette (France)

(Received July 16th, 1974)

(Revised manuscript received October 10th, 1974)

SUMMARY

The structure of the retinal rod disc membrane and its modifications upon bleaching have been studied by X-ray diffraction. Three types of preparations are used: functioning isolated frog retina, isolated rods from frog retina, oriented by a magnetic field, and stacked discs from cattle retina. X-rays are detected by a position-sensitive linear counter. Diffraction spectra are obtained in 10–100 s.

The electron density profile favors models where the rhodopsin molecule spans the whole thickness of the membrane. Upon bleaching, a small increase of electron density appears instantly at the cytoplasmic edge of the membrane. In the intact retina this structural change is accompanied by disorder and slow swelling reactions which are not observed in the isolated rod outer segment.

The diffraction signal arising from the protein distribution in the plane of the membrane has been reinvestigated carefully. Patterns identical to those of Blasie (Blasie (1969) J. Mol. Biol. 39, 407 and Blasie (1972) Biophys. J. 12, 191) can be obtained but these are shown to be dominated by artefacts. The actual signal is a single broad band around $(55\ \text{Å})^{-1}$, upon which bleaching has a negligible effect. No measurable displacement of rhodopsin in the thickness of the membrane occurs upon bleaching.

Temperature effects on the protein distribution are found to be large only for disc membranes from cattle retina. In this material from a warm-blooded animal those effects are correlated with the occurrence, upon lowering the temperature, of a partial phase transition of the paraffin chains of the lipids. The position and the slope of the transition are not sensitive to bleaching.

INTRODUCTION

The vertebrate retinal rods, site of the primary events leading to visual excitation, present many features which make them a particularly suitable material for membrane studies: the cell has attained a high degree of segregation, concentrating in the outer segment the disc membranes with their unique function of light detection. The outer segment can be easily broken off from the retina, thus yielding large quanti-

ties of pure membranes of great biochemical simplicity: one protein species, rhodopsin, accounts for about 85 % of the membrane's total protein content [1]. The quasi-crystalline ordering of the disc membranes in the native cell make them very suitable for studies by X-ray diffraction. Such studies have been performed in vivo [2], on dissected functioning retina [3], on strips of retina [4–6], on stacked discs [7, 8] and on artificially reconstituted rhodopsin/lipid/water systems [9]. However, from this large amount of work no clear picture has yet resulted of the membrane structure and of its modification upon bleaching the rhodopsin. Conflicting models exist for the shape of rhodopsin and for its location with respect to the membrane bilayer [4, 5, 7, 8]. The only point of agreement seems to be that the rhodopsin molecules are dispersed in the plane of the membrane without any special ordering, i.e. as a two-dimensional liquid [4, 7, 10]. This is confirmed by spectroscopic measurements of the freedom of rotation [11, 12], and the lateral diffusion [13, 14] of rhodopsin in the plane of the membrane.

The reason to try the X-ray diffraction approach again was the introduction of new improvements in the X-ray detection technique and in the material preparation. A new linear position-sensitive proportional counter allows a considerable shortening of the exposure times [15]. Measurable spectra are recorded in 10–100 s instead of the hour required with film techniques. This allows one to work on better controlled preparations and to isolate instantaneous light-induced structural changes from subsequent slow evolution or degradation. The first results obtained on isolated excitable retina have already been reported [3]. The work is extended here to isolated rods oriented by a magnetic field. This orientating effect has been observed [16] and explained [17] some years ago. It results from the preexisting parallel alignment of the 10^9 rhodopsin molecules within one rod. Such oriented preparations of isolated rods yield higher diffracted intensities than the intact retina. We are thus able to compare the changes obtained upon bleaching the isolated rods to those observed with the intact cells, and try to analyse which part of the photic response previously observed on the intact cells was specifically due to the outer segment, and which part resulted from the reaction of the whole cell.

The intense and highly oriented diffraction from rods in the magnetic field was also used to reinvestigate carefully the equatorial diffraction pattern. This diffraction originates from the molecular organisation in the plane of the membrane. Our results do not agree with the previous study and elaborate analysis of Blasie [7, 8, 18, 19]. The origin of the discrepancy is determined. The study was extended to the rod discs of cattle retina, to observe temperature effects which are expected to be important in membranes of a warm-blooded animal.

Only disc membrane structures and structural changes upon illumination are discussed here. Lattice changes and osmotic properties are presented in the next paper [20].

MATERIAL AND METHODS

Three types of material were prepared: isolated frog (*Rana esculenta*) retina, isolated outer segments from frog retina oriented in a magnetic field, and discs from bovine rod outer segments stacked and oriented by ultracentrifugation. Various diffraction geometries were used. The detection was based on the use of the position-

sensitive counter, but the orientation and the overall diffraction pattern were checked with films, generally after the counter measurement had been completed. All operations, unless specified, were carried out under dim red light. For bleaching and test illumination the light from a 30-watt tungsten lamp, set at 15 cm from the sample, was filtered through a cold filter. Diffraction measurements were performed in absolute darkness. The composition of the Ringer solution was (in mM): NaCl 101.8; KCl, 2.7; $MgCl_2$ 2.1; $CaCl_2$ 1.9; $NaHCO_3$ 2.0; NaH_2PO_4 0.36; pH adjusted at 7.4.

Apparatus

The Copper K_α X-rays were produced by Eliott rotating anode generators, run at 35 kV, 28 mA with a 0.1 × 1 mm focus for the work on isolated retina, and run at 30 kV, 50 mA with a 0.2 × 2 mm focus, otherwise. The generators have their cathode vertical and the front end window was used for linear beams, thus reducing the width of the object source to 10–20 microns. Linearly focused beams were produced either by an horizontal gold plated mirror and filtered by a 0.02 mm thick Ni foil, or by a Ni plated mirror without filtering. For point focusing a mirror monochromator combination was used.

For the orientation of the rods we had checked that the magnetic field homogeneity is of no importance, field gradients having no effect. The rod outer segment could then be oriented by a small (9 × 20 × 28 cm) permanent magnet mounted directly

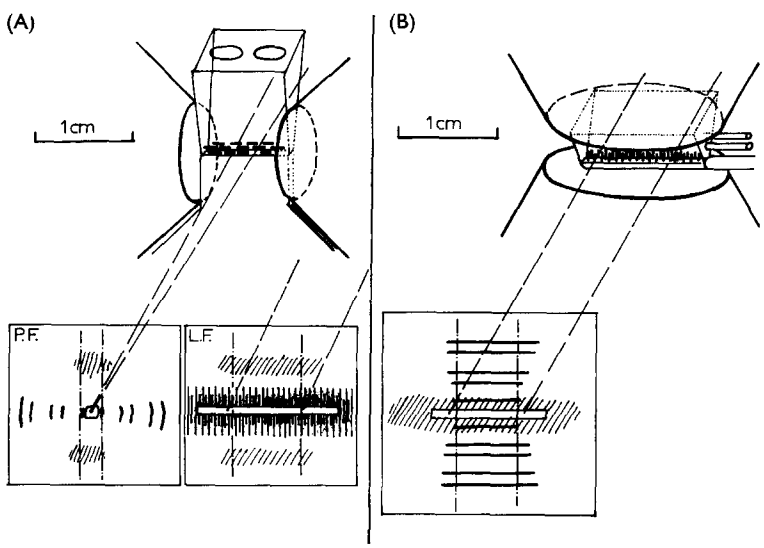

Fig. 1. Orientation of frog rod outer segments in a magnetic fiel (Ad.) Horizontal field: the rods, sedimented by gravity, are symbolised by the short horizontal bars at the bottom of the cell. X-ray diffraction patterns are sketched as they would appear on films. PF indicates point focusing and LF linear focusing. - -, X-ray beams; - · - · -, lateral limits of the counter entrance window. Hatching indicates diffuse scattering and bars sharp reflexions. The sharp 'meridional' lamellar reflexions observed with point focus appear as a diffuse signal with a linear focus. (B) Vertical field and horizontal linear focusing; the peaks of lamellar diffraction are sharp and symmetrical (see Fig. 3), and the equatorial diffraction appears only as a smooth background under the first orders of lamellar diffraction.

on the X-ray diffraction bench. The field, of 12800 Gauss, could be directed vertically or horizontally (Fig. 1). The position-sensitive linear detector [15, 21] has an active length of 60 mm, a width of 8 mm and a quantum efficiency of 60 % with xenon-methane (90 %–10 %) filling at atmospheric pressure. Linear resolution was 0.2 mm over the full length. The electronics were similar to those described earlier (3). The sample to detector distance varied between 15 and 28 cm depending on the measurement. These distances are longer than usual with films, and are chosen in order to optimise the use of the position-sensitive detector. With a film, a high background is given by its chemical fog and the signal: noise ratio is higher the shorter the sample to film distance. One is limited only by the beam size. With a counter, however, there is no background, so the sample to counter distance can be increased to improve the resolution. There is no loss of intensity as long as all the photons one is interested in fall within the limits of the counter window. A vacuum chamber was inserted between the sample and the detector. For work with the linear focused beam, the counter was set vertically and its full width was used to maximise the counting rate. With the point-focused beam an adjustable slit fixed on the counter was set to a smaller width (2–3 mm), and the counter was set on a rotatable stand. Then by simply rotating the detector by 90° one could measure equatorial and axial diffraction with the same calibration.

Sample preparation

The isolated retina preparation has already been reported [3]. At room temperature a Ringer-perfused retina kept its normal electrical response to light flashes for up to 6 h.

Isolated rod outer segments. Retina from 2 to 3 dark-adapted frogs were dissected in Ringer solution. The outer segments were detached from the retina by gentle shaking with a spatula for 30 s. The liquid was filtered through gauze and deposited on top of 2 % (w/w) Ficoll in Ringer solution. A first centrifugation, 40 s at $150 \times g$ sedimented pigment epithelium fragments and other fragments larger than the rods. The supernatant was transferred to another tube and the rods were sedimented for 100 s at $200 \times g$; in some cases another centrifugation was made to remove the Ficoll. The final supernatant was removed except for 100 μl of solution in which the rods were resuspended. Controls by microscopic observation showed that the preparations were very pure in the outer segments, the greater part of them appearing intact, with a length of 40–50 μm. On a few of them a part of the inner segment remained attached through the connecting cilium. The isolated rods in suspension, transferred to the sample holder in the magnetic field, were in the X-ray beam within 10 min from their detachment from the retina. A microscope was set on the bench to check the orientation directly in the sample holder. The rods aligned instantaneously in the field and kept their orientation even when the solution was stirred. In the vertical fieldconfiguration, due to their orientation all of the rods sedimented in less than 2 min to the bottom of the container, where they stacked as a brush. 90 % of the liquid in the container could then be pumped out and another solution could be reinjected and mixed by stirring with the remaining 10 %, thus creating an osmotic shock or any other desired change. This operation was performed in absolute darkness. In the horizontal field geometry the rods sedimented much slower, 5–10 min were necessary before stable counting rates were obtained; but if only relative intensities and positions

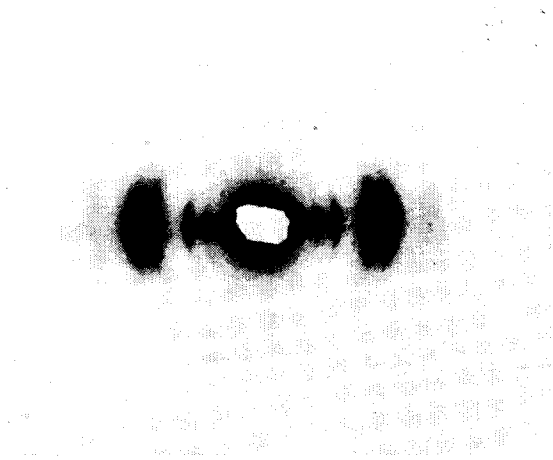

Fig. 2. X-ray diffraction film of oriented rods. The geometry is that of Fig. 1A with point focus. The "equatorial" diffraction is in the vertical direction to avoid interference with the parasitic scatter from the monochromator. Exposure 2 h, distance 15 cm. With longer exposure times a faint diffuse band is visible on the equator. The small arcing of the lamellar diffraction peaks is a check of the overall orientation of the sample. The angular spread is 32° (full width at half maximum). This spread is caused by irregular stacking of the rods at the bottom of the sample holder. When in diluted suspension, the rods are aligned with the field direction.

of diffraction peaks were needed, measurements could be started earlier. The solution could not be changed in this container; the temperature was controllable to within 1 °C between 6 °C and 35 °C.

The best check of orientation is provided by the diffraction patterns: Fig. 2 shows a film obtained with point focus and horizontal field (geometry 1A). This geometry, with the so-called "equatorial" diffraction recorded vertically was chosen when studying diffuse equatorial scattering, to avoid the contamination by parasitic scatter from the monochromator always present in the horizontal direction. Linear horizontal focus and vertical field (Fig. 1B) was the best geometry to study the lamellar reflexions. The counting rate was very high in this configuration, and the very existence of sharp symmetrical diffraction peaks was in itself a proof of the orientation. Linear horizontal focus with horizontal rod alignment (Fig. 1A) gave a strong equatorial signal. But with this geometry both the lamellar and the equatorial signals appeared as diffuse bands. If the orientation is not perfect the very intense lamellar diffraction may interfere with the equatorial signal. One should, therefore, be very careful when interpreting these data.

Stacked discs. Retina were dissected from dark-adapted cattle eyes. The rods were isolated by sucrose flotation, disrupted by an hypotonic shock and purified on a continuous sucrose gradient [9]. Repeated washings in distilled water were found necessary to obtain truly isolated discs. The discs tend to remain assembled in piles which do not align properly when stacked by centrifugation.

Two methods were used to prepare samples for diffraction; the first one was

according to Blasie [7]: a cylindrical lucite container (2 mm high, 6 mm diameter), closed at one end by a Mylar window, was fitted in a Spinco SW50 bucket. The disc suspensions were centrifuged for various times at more than 150 000 $\times g$. The container was then removed from the tube and sealed by another Mylar window, keeping an excess of water above the membrane pellet. It was set in a temperature-controlled holder and aligned so as to have the X-ray beam parallel to the sedimentation axis. This geometry did not provide any check on the sample orientation, even if a point-focused beam was used instead of the linearly focused beam. With perfectly oriented samples, only equatorial diffraction should be observed, but if the sample is only partially oriented, even with point focus, contamination of the stronger lamellar diffraction appears in the equatorial plane with the same cylindrical symmetry as the true equatorial diffraction.

Alternatively the samples were sedimented onto a mica strip 1 $\times$ 10 mm according to the method described by Dupont and Coll (22). After overnight centrifugation at 200 000 $\times g$ the membrane pellet was transferred to an airtight holder and set in a point focus beam with the sedimentation axis perpendicular to the beam. This geometry, equivalent to the geometry (1A) for the aligned rods, provided an internal check on the orientation. The water content of the sample could be reduced by letting the sample dry in the cold for short times.

RESULTS AND DISCUSSIONS

Lamellar diffraction

(*1*) *Structure of the disc membrane in the dark-adapted rods.* With isolated retina and isolated rods oriented in a magnetic field, the relative peak intensities of the lamellar diffraction patterns were very similar. For the isolated retina the counter sets an

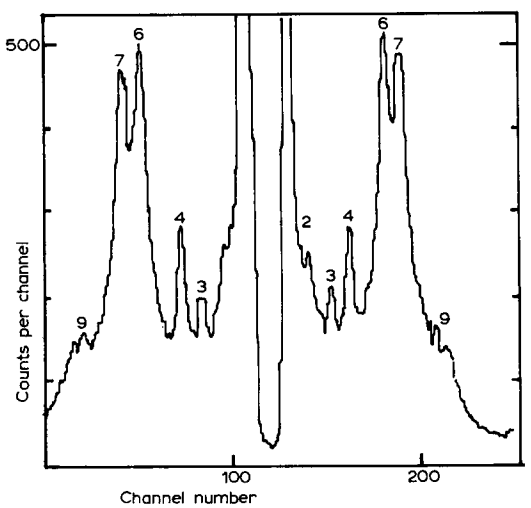

Fig. 3. X-ray diffraction spectrum of oriented rods. This spectrum was obtained with the counter in the geometry of Fig. 1B. Distance 25 cm. The lattice is 300 Å. Counting time 10 s. With this counting time the lattice variations are already measurable with a relative accuracy of the order of 0.5 %.

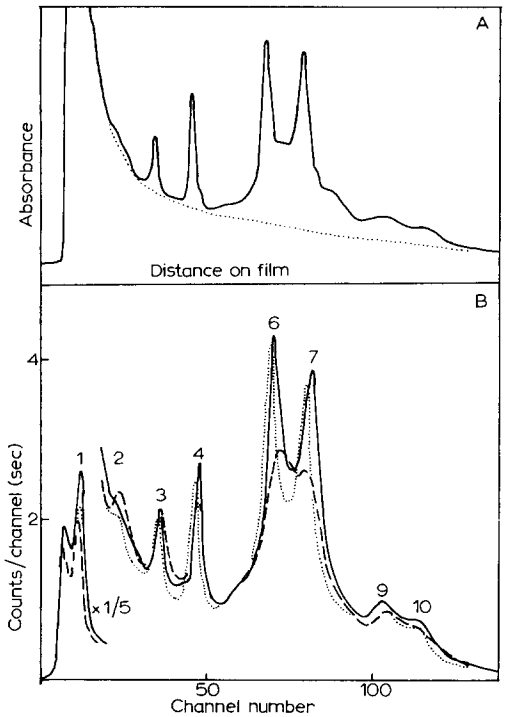

Fig. 4. Effect of bleaching on the lamellar diffraction in the isolated retina. (A) Densitometer tracing of a film placed in front of the counter, shown for comparison. Dark-adapted retina. Sample to film distance 28 cm. The lattice is 295 Å. (B) Spectra taken with the counter: —, dark-adapted retina; - - -, 5 min after bleaching; . . . . ., 100 min after bleaching. In the very first minutes after bleaching, the broadening of the peaks is too large to allow reliable intensity measurements. The broadening is still visible on higher orders after 5 min. Intensity changes are clear for orders 2 and 3. After 100 min, the lattice has changed, the peaks are as sharp as in the dark-adapted retina and the intensity changes seem to have reversed.

instrumental limit to the sharpness of the peaks (Fig. 4). For the latter preparation, higher counting rates are obtained but the peaks are somewhat broader.

The electron density profile of the disc membranes is obtained by Fourier synthesis from the amplitudes of the lamellar diffraction peaks, provided the correct phase is known for each reflexion. The phases were selected using the same procedure as Blaurock and Wilkins [10] and Corless [23], that is swelling experiments which change the lattice with, hopefully, little change to the disc structure. The electron density profile obtained (Fig. 6) is similar to that proposed by these authors but with a small assymetry toward the outer side of the membrane. The disagreement with the profile proposed by Worthington [24] is due more to a difference in the analysis than to differences in the data. Our electron density profile resembled that obtained with pure lipid bilayers. However, even without a knowledge of the absolute electron density scale one can notice a difference: the whole pattern is shifted upward with respect to the water level. The two high density peaks are larger than the low density dip at the center, the opposite being true for lipid bilayers [25]. The proteins, which

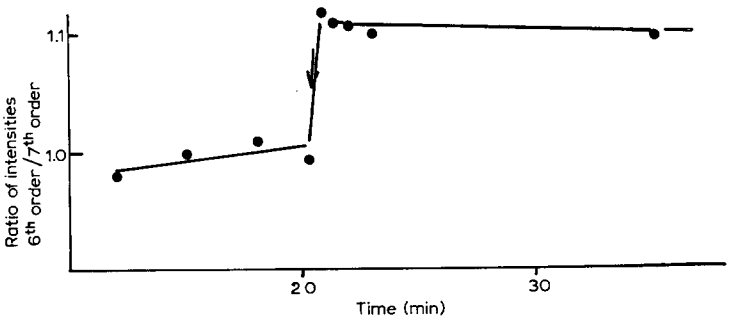

Fig. 5. Kinetics of the diffraction intensity changes upon bleaching, observed on isolated outer segments. The ratio of intensities of two diffraction peaks is plotted against time. The origin of the time scale is the time of separation of the rods from the retina. Arrow indicates the instant of illumination. The change is completed in less than 30 s.

account for more than half of the membrane weight, must cause this upward shift. The fact that the profile is nearly symmetrical suggests that the protein mass is distributed through the whole thickness of the membrane. The persistence of a pronounced dip at the center indicates that the protein is not concentrated there, but does not exclude the possibility that it could span the whole thickness of the membrane.

(*2*) *Effect of total bleaching.* On the isolated retina [3], total bleaching induced disorder and osmotic reactions which could partially mask the structural changes (Fig. 4). If the light intensity was such as to bleach the retina totally in less than 20 s, reliable diffraction measurements were not feasible during the first minutes, due to a broadening of the peaks. It was checked that this was not due to a heating of the retina

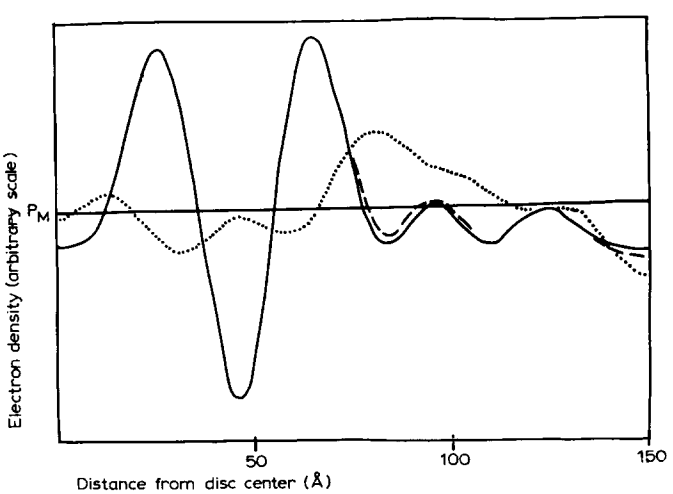

Fig. 6. Electron density profile of a rod disc, obtained from the lamellar diffraction spectrum. 10 orders have been included in the calculation with the following set of phase signs: + − + + + − − − + + . ———, Dark adapted; - - -, bleached; . . . . ., difference spectrum, enlarged fivefold. The main change is observed around 75 Å from the disc center, at the cytoplasmic edge of the disc membrane. A smaller, and unexplained change is also seen in the middle of the cytoplasmic region.

It was, therefore, difficult to ascertain whether all of the intensity changes measured later were instantaneous or were due to the subsequent slow lattice evolution.

With isolated rods, the broadening upon bleaching was less important, sometimes hardly noticeable, and the lattice remained stable after bleaching [20]. Accurate intensity measurements could be made within 30 s of bleaching. The intensity changes were instantaneous and stable (Fig. 5). For orders 2, 3, and 4 they were identical to those observed with intact retina, but in addition changes for orders 6, 7 and 9, not observable on the intact retina, appeared clearly with the isolated rods. The effect of those intensity changes on the electron density profile is not very spectacular (Fig. 6). Qualitatively we confirm the finding of Corless [23], which is an outward displacement of high electron density to the cytoplasmic side of the membrane, but the effect we find is smaller. The change is a maximum at the very edge of the membrane. If it is due to a structural modification of the rhodopsin molecules, it must occur in a part that extends into the aqueous phase. Rhodopsin is known to by phosphorylated upon bleaching with possibly up to 4 phosphorus sites per molecule [26]. This could be sufficient to account for the observed change. However, the phosphorylation is a dark reaction after bleaching with kinetics slower than those we observed. Within 1 h after bleaching, no evolution or reversion of the intensity changes could be detected with the isolated rods, in opposition to what is observed in the intact cell. A general slow decrease of all the diffraction peaks is observed with the isolated rods as if the material were slowly degrading. Bleached, isolated rods seemed far less stable than dark-adapted ones.

Equatorial diffraction

The diffraction observed in the equatorial direction is representative of the molecular organisation in the plane of the membrane. Two distinct ranges of reciprocal distances are of interest, the large angle range around $(4\text{Å})^{-1}$, which corresponds to the correlation distances between the paraffin chains of the lipids, and the small angle range, between $(25\text{ Å})^{-1}$ and $(100\text{ Å})^{-1}$, corresponding to electron density fluctuations of the order of the protein size and of interprotein distances.

(*1*) *Phase transition in the lipid paraffin chains.* Paraffin chains of the lipids can take two configurations: at physiological temperatures the chains are usually disordered and the paraffin region behaves as a two-dimensional liquid. At lower temperatures the chains may become rigidly ordered. In X-ray diffraction the liquid state is characterised by a broad band around $(4.5\text{ Å})^{-1}$ and the rigid state by a sharp line at $(4.15\text{ Å})^{-1}$. The phase transition is slow, smooth and never complete in lipid/protein/water systems and membranes [15]. The hydrophobic interaction of membrane proteins with lipids creates additional disorder and hinders the lipid lateral diffusion, hence the formation of ordered lipid regions. Since the protein lipid interaction is a limiting factor in the process, a change in the hydrophobic interaction of rhodopsin upon bleaching might act upon the temperature or slope of the transition. For this study we have used stacked discs from bovine retina because in warm-blooded animal membranes some rigidification may occur above 0 °C, whereas this is not expected in membranes from frogs.

A smooth phase transition is observed, starting below 20 °C. It involves, above our lower limit of 5 °C, only a small part of the lipids (Fig. 7). We have not tried to quantify the extent of rigidification, being only interested in an eventual

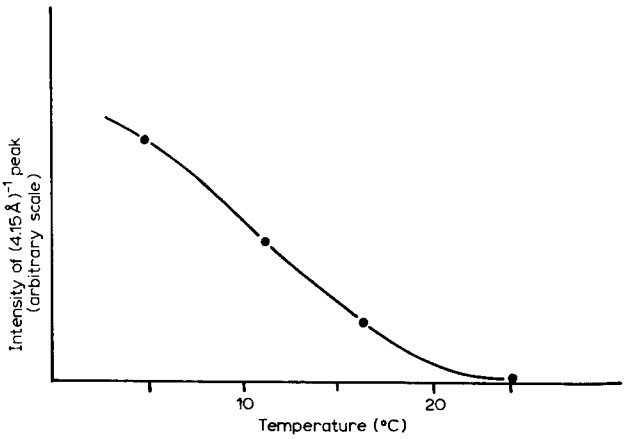

Fig. 7. Phase transition of the paraffin chains of the lipids in cattle disc membranes. The vertical scale is proportional to the intensity of the (4.15 Å)$^{-1}$ reflexion characteristic of ordered rigid paraffin chains. Even at 5 °C, this peak amounts only to a small part of the paraffin chains.

variation of the phenomenon upon the bleaching of rhodopsin, and no variation was observed. This implies that there is no major change in the protein lipid interaction upon bleaching. It could be that the method is not sensitive enough, but our results correlate well with the very small changes observed by the spin label technique upon bleaching for the ordering of the paraffin chains [27, 28].

(*2*) *Protein distribution in the plane of the membrane.* The small angle equatorial diffraction originating from the protein is also influenced by the lipid behavior: any lipid segregation also implies a correlated segregation of the proteins, which can be seen by freeze-etching electron microscopy [29]. We wanted to verify this effect and also to check previous contradictory X-ray diffraction results [7, 10]. Blasie and his collaborators [7, 8, 18, 19] have given an elaborate analysis of their results, with precise conclusions as to the shape of rhodopsin, its distribution in the plane of the membrane and its location on the external side. A few remarks may be made on this type of analysis. (a) If the distances between the protein molecules are of the same order of magnitude as their size, which seems the case here, shape diffusion by the molecule and interparticle correlations both contribute to the diffraction in the same range. There is no way to distinguish between the two contributions unless one could vary the protein concentration. It is only by arbitrarily assuming a shape for the molecule that one might try to calculate a distribution. The temperature dependence of the diffraction pattern, however, may be attributed entirely to changes in the distribution by assuming the shape of the protein to be insensitive to temperature. (b) The equatorial diffraction is related only to the projection of the protein molecule onto the plane of the membrane. Since rhodopsin molecules are free to rotate only around an axis perpendicular to the membrane [11, 30, 31] there is no information as to the extension of the molecule in the direction perpendicular to the membrane. (c) In a quantitative analysis one should not neglect the phosphate region of the lipids which has an electron density very different from that of water and of the paraffin region. There is no ex-

perimental information about the relative contribution of the different components to the diffraction.

The equatorial small angle diffraction was first measured on stacked discs from bovine retina, using the same method for sample preparation and the same geometry as Blasie, i.e. an X-ray beam parallel to the sedimentation axis. The patterns obtained were similar to that of Blasie with two smooth maxima around $(80\ \text{Å})^{-1}$ and $(50\ \text{Å})^{-1}$. Since this geometry does not provide any check on the orientation another geometry was used to check whether the pattern actually originated from equatorial diffraction. The sample, a slice of the previous one, or prepared according to the other method (see Methods) was set with its sedimentation axis perpendicular to a point focus X-ray beam. Even after overnight centrifugation, as long as one kept an excess of water over the pellet the ordering and the orientation were poor. In the meridional direction a broad intensity pattern which resembled the continuous Fourier transform of the disc profile, with maxima around $(80\ \text{Å})^{-1}$ and $(50\ \text{Å})^{-1}$ was observed. The arking of this meridional diffraction intercepted the equatorial direction. It was only by removing the excess water and air drying until the water content was no more than 50 % w/w, that better orientation and sharp lamellar diffraction were obtained. When strongly overexposing the meridional reflexions, a faint broad equatorial band around $(55\ \text{Å})^{-1}$ could be observed. We, therefore, interpret the pattern observed with the beam axis parallel to the sedimentation axis as due to the superposition of an equatorial signal at $(55\ \text{Å})^{-1}$ and diffuse lamellar diffraction.

For frog rods, the more reliable orientation procedure by a magnetic field allowed us to work on intact cells in suspension in Ringer. To obtain an accuracy of a few percent on the diffraction pattern, 5–10 min. were sufficient with a linearly focused beam (geometry 1 A) against 2–3 h with a point focus beam. But this last geometry provided the necessary controls of orientation. The pattern obtained with this material confirms our finding on the stacked discs from cattle retina: on a smooth decreasing curve only one broad band around $(55\ \text{Å})^{-1}$ can be seen. It follows from our preliminary discussion that the only information that we think can be reliably deduced from these data is the absence of crystalline order for the proteins in the plane of the membrane.

Total bleaching did not produce very significant changes on the small angle diffraction, either for cattle stacked discs or for frog oriented rods. Local intensity changes were within 3 %. Whenever a noticeable increase of intensity was observed upon bleaching, in the range from $(100\ \text{Å})^{-1}$ to $(30\ \text{Å})^{-1}$ checks indicated the appearance of an unoriented diffraction ring around $(60\ \text{Å})^{-1}$ probably due to lipids released from the membranes. With a linear focus, only an increase of intensity is seen in this range, and this may be misinterpreted as a change due to the proteins.

Temperature effects on the small angle equatorial diffraction were small for the frog rods but larger for cattle rod discs. On the patterns obtained with the stacked discs, known to be contaminated by lamellar diffraction, important and reversible variations with temperature were observed (Fig. 8A). Having checked that the meridional diffraction was hardly affected by temperature, the variation may be interpreted as arising from the underlying true equatorial diffraction. Upon lowering the temperature there was as shift of the diffracted intensity as would be given by a shift of an underlying band at $(57\ \text{Å})^{-1}$ toward larger angles. But the changes were not confined to this region and were also observed at smaller angles. With the detector and line focus geometry each measurement lasted only 5 min and the revers-

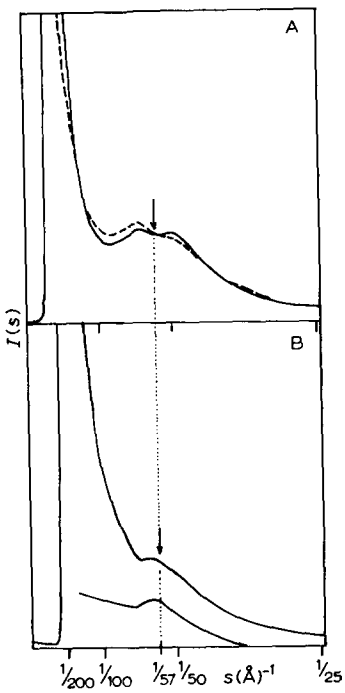

Fig. 8. Small angle equatorial scattering. (A) Pattern obtained with stacked discs of cattle retina centrifuged for 2 h at 150 000 × g and kept with an excess of water. The beam axis was parallel to the centrifugation axis (geometry of Blasie et al. [7]). The two bumps around $(80\,Å)^{-1}$ and $(50\,Å)^{-1}$ originate from contamination by lamellar diffraction (see text). The arrow indicates the position of the underlying equatorial band; as it is observed at laboratory temperature with the point focus beam perpendicular to the sedimentation axis, and when the sample orientation is improved by reducing the water content. —, 5 °C; - - -, 40 °C. The changes are totally reversible for measurements not exceeding 10–15 min. Changes upon bleaching are negligible on this scale. (B) Pattern obtained at room temperature with oriented rods from frog retina. Diffraction geometry is that of Fig. 1A with point focus and vertical counter. The lower curve is obtained by subtracting the background measured with the sample cell filled with water. Changes upon bleaching are not visible on this scale, and temperature effects are also too small in comparison with the thickness of the line.

ibility was always checked over this period. Over longer periods, however, reproducibility was not perfect, but the difference spectrum for two successive measurements at two given temperatures remained constant. This agrees with our interpretation that the spectra were contaminated by long term artefacts, but that the short time temperature effects were mostly due to the true equatorial diffraction. There is a reduction of the correlation distance between the proteins when lowering the temperature. This must be correlated with the existence in this material of a phase transition for the lipids: the formation of ordered patches of lipids implies a segregation of the proteins.

CONCLUSIONS

With our improved techniques, the conclusions will be safer but not necessarily more elaborate than previous ones. In some respects it even seems that we have re-

gressed, by questioning previous work, particularly on the structural variations upon bleaching.

Our electron density profile indicates only that rhodopsin is distributed throughout the entire thickness of the membrane with only a slight assymetry toward the cytoplasmic side. The functional asymmetry of the membrane leads us to reject models where the rhodopsin molecules are distributed as two populations on both sides of the membrane. The model we prefer is the one where rhodopsin, an elongated protein, spans the whole thickness of the membrane. This is in agreement with the only published result bearing directly on the shape of rhodopsin [32] and evidence by freeze-etching techniques that the protein is deeply embedded in the lipid matrix of the membrane and that it remains anchored to the outer side when the membrane splits [33, 34]. Our model would, therefore, be similar to that proposed recently by Cone and Szuts [35], with a hydrophobic rod connecting two parts situated on both sides of the membrane.

Upon bleaching, changes in the lamellar diffraction indicate a small but definite increase of electron dense material at the cytoplasmic edge of the membrane, in agreement with the previous observation of Corless [23]. The kinetics of appearance of this change seem too fast to attribute this effect to the phosphorylation of rhodopsin after bleaching.

Our reinvestigations of the diffraction arising from the protein distribution in the plane of the membrane leads to a serious questioning of Blasie's results and interpretation. We agree only on the fact that the proteins are dispersed in the plane without any regular ordering. The equatorial signal is a single broad band around $(55\,\text{Å})^{-1}$, and bleaching has no measurable effect on it. There is, therefore, no evidence of a displacement of the rhodopsin molecule within the thickness of the disc membrane when it is bleached.

Effects of temperature on the protein distribution in the plane of the membrane are negligible for frog rods. For rod disc membrane from cattle, a warm-blooded animal, the lowering of temperature induces a partial phase transition of the lipids and a correlated segregation of the proteins.

ACKNOWLEDGEMENTS

I thank A. Gabriel for providing the position-sensitive detectors, A. Cavaggioni and T. Gulik Krzywicki for discussions and for their participation in some of the measurements and V. Luzzati for welcoming me in his laboratory where this work was initiated and for his stimulating criticisms. This work was supported in part by a grant from the Délégation Générale à la Recherche Scientifique et Technique, comité des membranes biologiques. The author is on the staff of C.N.R.S.

REFERENCES

1 Bownds, D., Gordon-Walker, A., Gaide-Hugenin, A. C. and Robinson, W. (1971) J. Gen. Phys. 58, 225–237
2 Webbs, N. G. (1972) Nature 235, 44–46
3 Chabre, M. and Cavaggioni, A. (1973) Nat. New Biol. 244, 118–120
4 Blaurock, A. E. and Wilkins, M. H. F. (1969) Nature 223, 906–909
5 Gras, W. J. and Worthington, C. R. (1969) Proc. Natl. Acad. Sci. U.S. 63, 233–238

6 Corless, J. M. (1971) Thesis, Duke University
7 Blasie, J. K., Worthington, C. R. and Dewey, M. M. (1969) J. Mol. Biol. 39, 407–416
8 Blasie, J. K. and Worthington, C. R. (1969) J. Mol. Biol. 39, 417–434
9 Chabre, M., Cavaggioni, A., Osborne, H. B., Gulik Krzywicki, T. and Olive, J. (1972) FEBS Lett. 26, 197–202
10 Blaurock, A. E. and Wilkins, M. H. F. (1972) Nature 236, 313–314
11 Cone, R. A. (1972) Nat. New Biol. 236, 39–43
12 Brown, P. K. (1972) Nat. New Biol. 236, 35–38
13 Poo, M. and Cone, R. A. (1974) Nature 247, 438–441
14 Liebman, P. A. and Entine, G. (1974) Science 185, 457–459
15 Dupont, Y., Gabriel, A., Chabre, M., Gulik Krzywicki, T. and Schechter, E. (1972) Nature 238, 331–333
16 Chalazonitis, N., Chagneux, R. and Arvanitaki, A. (1970) C. R. Acad. Sci., Paris, 271 D, 130–133
17 Hong, F. T., Mauzerall, D. and Mauro, A. (1971) Proc. Natl. Acad. Sci. U.S. 68, 1283–1285
18 Blasie, J. K. (1972) Biophys. J. 12, 191–204
19 Blasie, J. K. (1972) Biophys. J. 12, 205–213
20 Chabre, M. and Cavaggioni, A. (1975) Biochim. Biophys. Acta 382, 336–343
21 Gabriel, A. and Dupont, Y. (1972) Rev. Sc. Inst. 43, 1600–1603
22 Dupont, Y., Harrison, S. C. and Hasselbach, W. (1973) Nature 244, 555–558
23 Corless, J. M. (1972) Nature 237, 229–231
24 Worthington, C. R. (1973) Exp. Eye Res. 17, 487–503
25 Luzzati, V., Tardieu, A. and Taupin, D. (1972) J. Mol. Biol. 64, 269–286
26 Bownds, D., Brodie, A., Robinson, W. E., Palmer, D., Miller, J., and Sheldowski, A. (1974) Exp Eye Res. 18, 253–269
27 Verma, S. P., Berliner, L. J. and Smith, I. C. P. (1973) Biochem. Biophys. Res. Commun. 55, 704–709
28 Hong, K. and Hubbell, W. L. (1972) Proc. Natl. Acad. Sci. U.S. 69, 2617–2621
29 Chen, E. S. and Hubbell, W. L. (1973) Exp. Eye Res. 17, 517–527
30 Schmidt, W. J. (1938) Kolloidzeitschrift 85, 137–148
31 Denton, E. J. (1954) J. Physiol. 124, 17–18
32 Chen-Wen, W. and Stryer, L. (1972) Proc. Natl. Acad. Sci. U.S. 69, 1104–1108
33 Corless, J. M., Costello, J. and Cobbs, W., J. Cell. Biol., in the press
34 Olive, J. and Benedetti, E. L. (1974) Mol. Biol. Reports 1, 245–249
35 Cone, R. A. and Szuts, E. (1973) Exp. Eye Res. 17, 507–510